Supplemental Figures

Figure S1

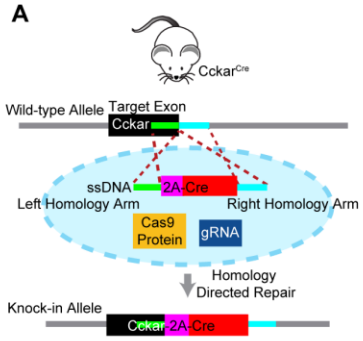

B Sequence information

gRNA sequence

gagctgtacctggttcgctg

ssDNA sequence

ggtgagaggagaagtgggagaggaggaagatggaaggaccataagggcatccctgtcccggtattcctacagccaca
tgagcacctctgccccaccccacggttccggagagggcagaggaagtcttctaacatgcggtgacgtggaggagaatc
ccggccctatgtccaatttactgaccgtacaccaaaatttgcctgcattaccggtcgatgcaacgagtgatgaggttcgcaa
gaacctgatggacatgttcagggatcgccaggcgttttctgagcatacctggaaaatgcttctgtccgtttgccggtcgtggg
cggcatggtgcaagttgaataaccggaaatggtttcccgcagaacctgaagatgttcgcgattatcttctatatcttcaggcg
cgcggtctggcagtaaaaactatccagcaacatttgggccagctaaacatgcttcatcgtcggtccgggctgccacgacc
aagtgacagcaatgctgtttcactggttatgcggcggatccgaaaagaaaacgttgatgccggtgaacgtgcaaaacag
gctctagcgttcgaacgcactgatttcgaccaggttcgttcactcatggaaaatagcgatcgctgccaggatatacgtaatct
ggcatttctggggattgcttataacaccctgttacgtatagccgaaattgccaggatcagggttaaagatatctcacgtactg
acggtgggagaatgttaatccatattggcagaacgaaaacgctggttagcaccgcaggtgtagagaaggcacttagcct
gggggtaactaaactggtcgagcgatggatttccgtctctggtgtagctgatgatccgaataactacctgttttgccgggtca
gaaaaaatggtgttgccgcgccatctgccaccagccagctatcaactcgcgccctggaagggatttttgaagcaactcatc
gattgatttacggcgctaaggatgactctggtcagagatacctggcctggtctggacacagtgcccgtgtcggagccgcgc
gagatatggcccgcgctggagtttcaataccggagatcatgcaagctggtggctggaccaatgtaaatattgtcatgaact
atatccgtaacctggatagtgaaacaggggcaatggtgcgcctgctggaagatggcgatt***gagctgtacctggttcgct***
gcgagcagcagaaaggaggggactgggagcaaggaggaagaggaagtgggagggaaggagaaggaagaccc
atttc

Green: 5' homology arm; Magenta, T2A; Red: Cre; Cyan: 3' homology arm.

NOTE: PAM site within the HR template was mutated from CGG to CGA to protect the HR template from Cas9.

Figure S1. Generation of Cckar^{Cre} mice. Related to Figure 1

(A) Strategy for inserting 2A-Cre into the *Cckar* locus using CRISPR/Cas9-mediated homologous recombination (HR).

(B) Sequence information of gRNA and single-stranded DNA (ssDNA).

Figure S2

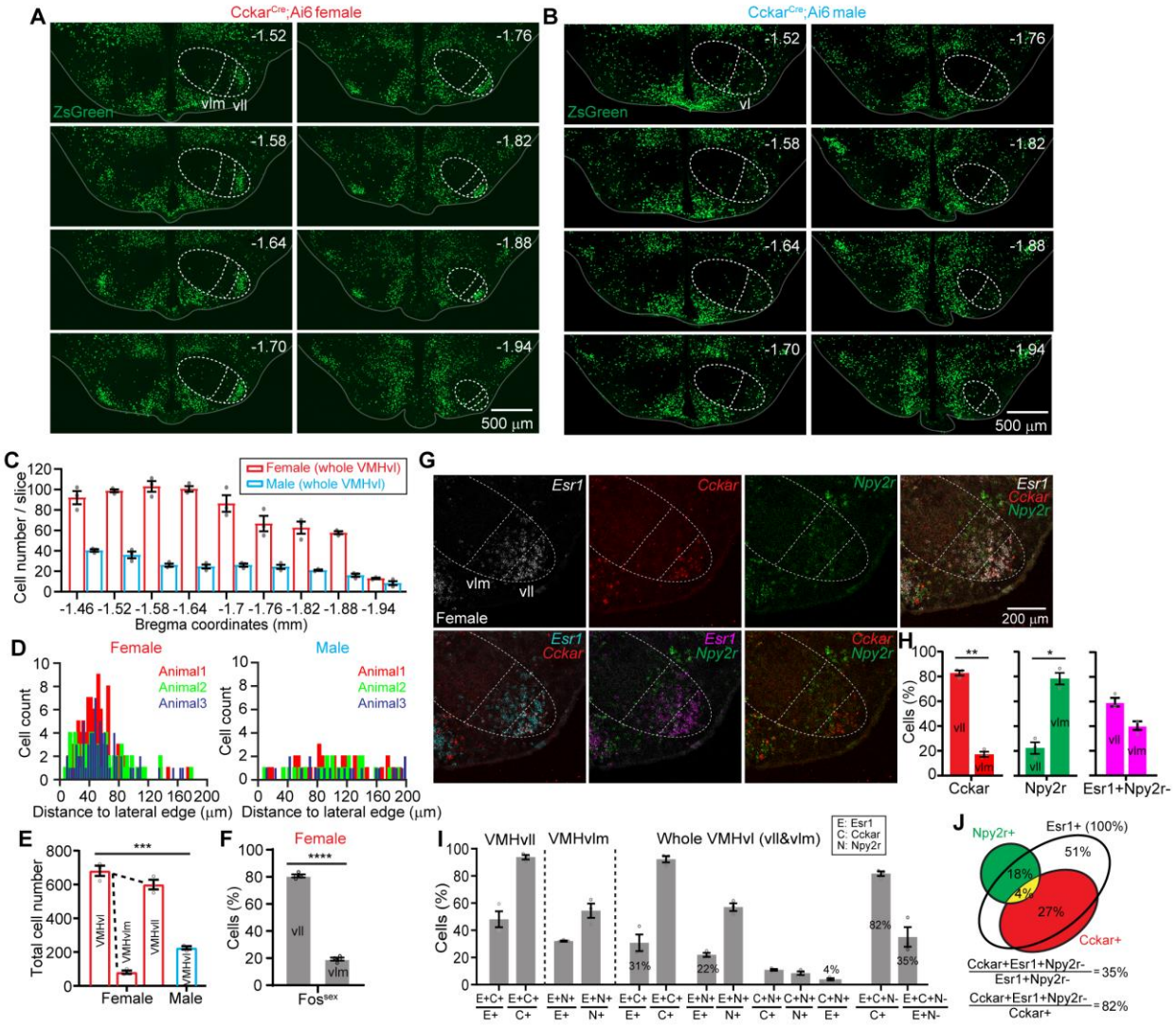

Figure S2. Sexually dimorphic expression of Cckar in the VMHvl and the relationship of *Cckar, Esr1* and *Npy2r* in female VMHvl. Related to Figure 1

(A) The distribution of ZsGreen cells at different Bregma levels along the anterior-posterior axis of the VMH from a Cckar^{Cre};Ai6 female mouse. Dotted lines indicate VMH subdivisions.

(B) The distribution of ZsGreen cells in the VMH of a male Cckar^{Cre};Ai6 mouse.

(C) Quantification of (B) and (C) in the whole VMHvl from Bregma -1.46 mm to -1.94 mm.

(D) Distribution of the distance of Cckar cells to the lateral edge of VMH from three females (left) and three males (right).

(E) The total numbers of Cckar+ cells in female VMHvl, VMHvlm and VMHvll, and male VMHvl.

(F) The distribution of Fos^{Sex} cells in the female VMHvll and VMHvlm.

(G) Representative images showing expression of *Esr1, Cckar,* and *Npy2r* mRNA. Cckar (red), Npy2r (green), Esr1 color is changed when overlaid with different genes for better visualization.

(H) Proportions of Cckar (red), Npy2r (green) and Esr1+Npy2r- (magenta) cells in the lateral- (vll) vs. medial- (vlm) subdivisions of VMHvl.

(I) The overlap between different populations of cells. The numbers used in (J) are highlighted inside of the bars.

(J) (Top) The overlap between Npy2r+&Cckar+, Npy2r+&Esr1+, Cckar+&Esr1+ among the whole VMHvl Esr1+ cells. (Bottom) the overlap between Cckar+& Esr1+Npy2r- cells.

Data are mean ± s.e.m. (E) Two-tailed unpaired t test. (F, H) Two-tailed paired t test. *p<0.05; **p<0.01; ***p<0.001; ****p<0.0001.

n = number of animals. n=3 (C, E, H, I), n=4 (F) females.

Figure S3

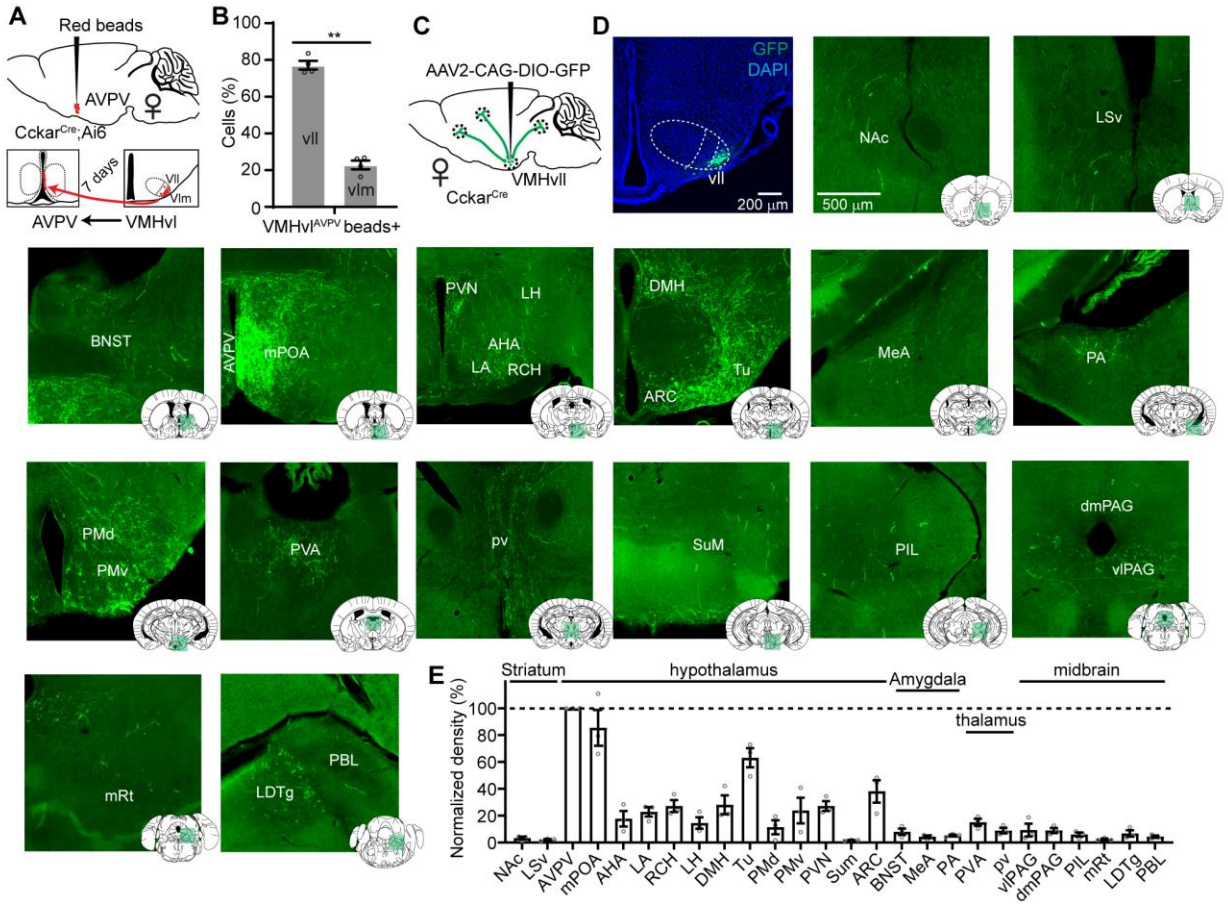

Figure S3. The projection pattern of female VMHvll^{Cckar} cells. Related to Figure 1

(A) Injection of red retrobeads into AVPV to retrogradely label VMHvl cells.

(B) The distribution of beads+ cells in female VMHvll and VMHvlm 7 days after injection.

(C) Viral strategy for axon tracing of female VMHvll^{Cckar} cells.

(D) Representative images showing GFP expressing VMHvll^{Cckar} cells and their axon terminals in various brain regions of a female mouse.

(E) Quantification of GFP^{+} fiber density in various brain regions.

NAc, nucleus accumbens; LSv, lateral septum ventral part; BNST, bed nucleus of stria terminalis; AVPV, anteroventral periventricular nucleus; mPOA, medial preoptic area; PVN, paraventricular nucleus of the hypothalamus; LH, lateral hypothalamus; AHA, anterior hypothalamic area; LA, lateroanterior hypothalamic nucleus; RCH, retrochiasmatic area; DMH, dorsomedial hypothalamic nucleus; ARC, arcuate hypothalamic nucleus; Tu, tuberal nucleus; MeA, medial amygdala; PA, posterior amygdala; PMd, dorsal premammillary nucleus; PMv, ventral premammillary nucleus; PVA, paraventricular thalamic nucleus, anterior part; pv, periventricular fiber system;

SuM, supramammillary nucleus; PIL, posterior intralaminar thalamic nucleus; dmPAG, dorsomedial periaqueductal gray; vlPAG, ventrolateral periaqueductal gray; mRt, mesencephalic reticular formation; LDTg, laterodorsal tegmental nucleus; PBL, lateral parabrachial nucleus;

Data are mean ± s.e.m. (B) Two-tailed paired t test. $^{**}p<0.01$.

n = number of animals. n=4 (B), n=3 (E) females.

Figure S4

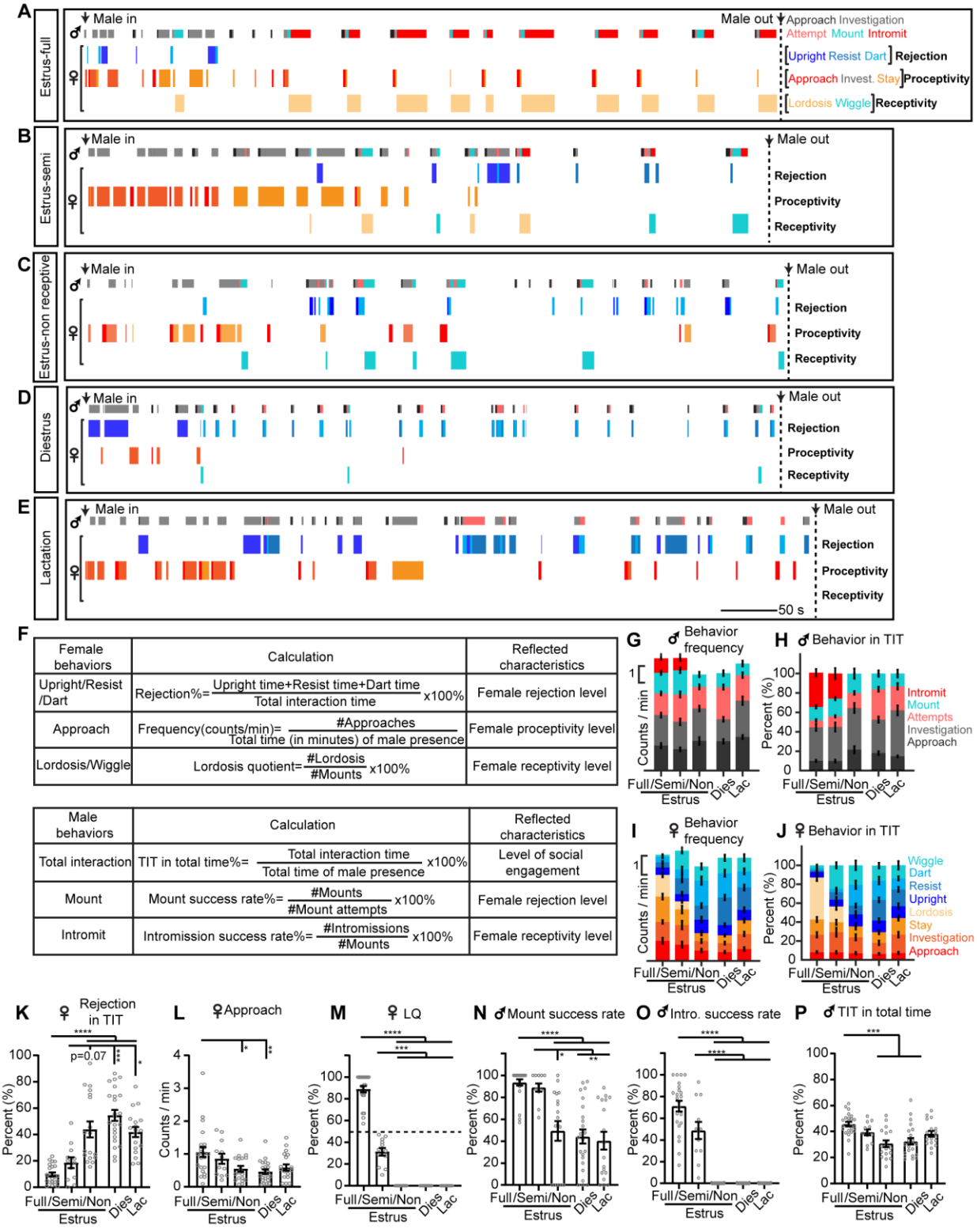

Female behaviors	Calculation	Reflected characteristics
Upright/Resist /Dart	$\text{Rejection\%}=\frac{\text{Upright time+Resist time+Dart time}}{\text{Total interaction time}}\times 100\%$	Female rejection level
Approach	$\text{Frequency(counts/min)}=\frac{\text{\#Approaches}}{\text{Total time (in minutes) of male presence}}$	Female proceptivity level
Lordosis/Wiggle	$\text{Lordosis quotient}=\frac{\text{\#Lordosis}}{\text{\#Mounts}}\times 100\%$	Female receptivity level

Male behaviors	Calculation	Reflected characteristics
Total interaction	$\text{TIT in total time\%}=\frac{\text{Total interaction time}}{\text{Total time of male presence}}\times 100\%$	Level of social engagement
Mount	$\text{Mount success rate\%}=\frac{\text{\#Mounts}}{\text{\#Mount attempts}}\times 100\%$	Female rejection level
Intromit	$\text{Intromission success rate\%}=\frac{\text{\#Intromissions}}{\text{\#Mounts}}\times 100\%$	Female receptivity level

Figure S4. Characterization of sexual behaviors of female mice at various reproductive states. Related to Figures 2 and 4

(A-E) Raster plots showing social behaviors of a pair of male and female mice during ~10 min free interaction. The females were in estrus (A-C), diestrus (D) or lactation (E) and showed varying levels of rejection, proceptivity and receptivity. All males were highly sexually experienced. Behaviors are-color coded.

(F) A table showing a list of analyzed female and male behaviors, the parameters used for quantification and the reflected characteristics of the females.

(G and I) The frequency of various behaviors expressed by males (G) and females (I) during male-female interaction, separated based on females' reproductive and receptive states.

(H and J) The percentage of time the male (H) and the female (J) expressing a specific behavior during the total interaction time (TIT), separated based on females' reproductive and receptive states.

(K) The percentage of time female spent on rejecting the male during the total interaction time for each of five groups of females.

(L) The frequency to female-initiated approach for each of the five groups.

(M) The LQ of each of the five groups of females.

(N) The mounting success rate of the male when paired with females from different groups.

(O) The intromission success rate of the male when paired with females from different groups.

(P) The percentage of time animals spent on interacting with each other during a recording session.

Data are mean ± s.e.m. (K-P) Kruskal-Wallis test with Dunn's multiple comparisons test. *p<0.05; **p<0.01; ***p<0.001; ****p<0.0001.

n = number of animals. (I-M, P) n=23, 12, 18, 23, 18 fully receptive estrous, semi-receptive estrous, non-receptive estrous, diestrous and lactating females, respectively. Numbers of males in (G-H, N-P) are the same as numbers of females in (I-M, P) for each group.

Figure S5

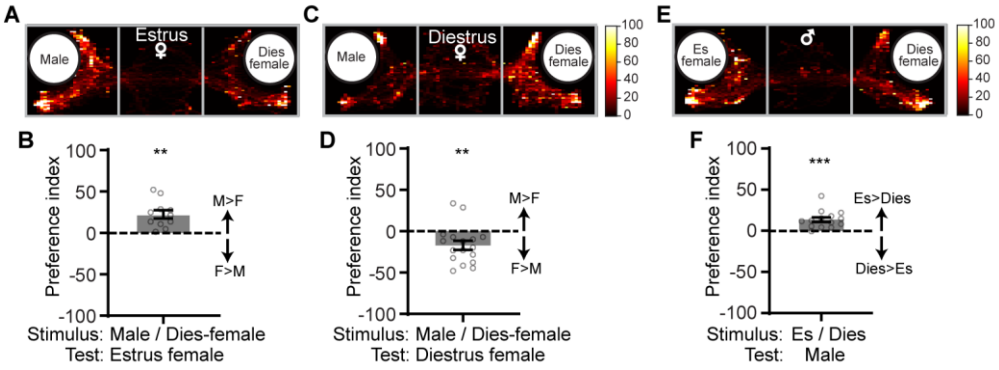

Figure S5. Social preference of male and female mice. Related to Figures 2 and 4

(A and C) Heatmap showing the distribution of female's body center location in a social preference test when the female is in estrus (A) or diestrus (C). Stimulus animals are a sexually experienced unfamiliar male and an unfamiliar diestrous female.

(B and D) Preference index in the social test of estrous (B) and diestrous females (D). PI = (time in male chamber - time in female chamber)/(time in male chamber + time in female chamber) × 100%.

(E) Heatmap showing the distribution of a male's body center location in a social preference test. Stimulus animals are an unfamiliar diestrous female and an unfamiliar estrous female.

(F) Preference index in the social test of sexually experienced males. PI = (time in estrous female chamber - time in diestrous female chamber)/(time in estrous female chamber + time in diestrous female chamber) × 100%.

Data are mean ± s.e.m. (B-F) One sample t test, with hypothetical value as 0. $^{**}p<0.01$; $^{***}p<0.001$.

n = number of animals. n = 11 (B), 17 (D) and 14 (F) animals.

Figure S6

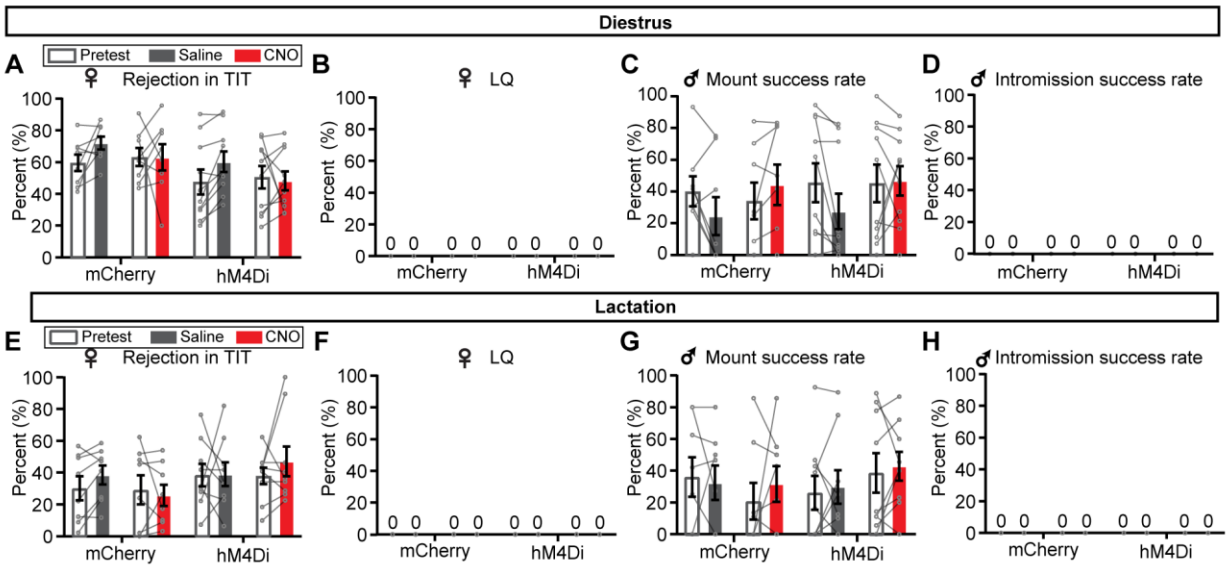

Figure S6. Inhibiting VMHvll^{Cckar} cells does not change sexual behaviors in diestrous and lactating females. Related to Figure 2

(A-D) In diestrous female, inhibiting VMHvll^{Cckar} cells does not change the percentage of total interaction time females spent on rejecting the males (summation of upright, resist and dart) (A), lordosis quotient (B), male mount success rate (C), and male intromission success rate (D).

(E-H) same as (A-D) but in lactating females.

Data are mean ± s.e.m. (A, C, E, G) Two-way ANOVA with Sidak's multiple comparisons test.

n = number of animals. n=8 for mCherry group, and n=10 (A-D), 9 (E-H) for hM4Di group.

Figure S7

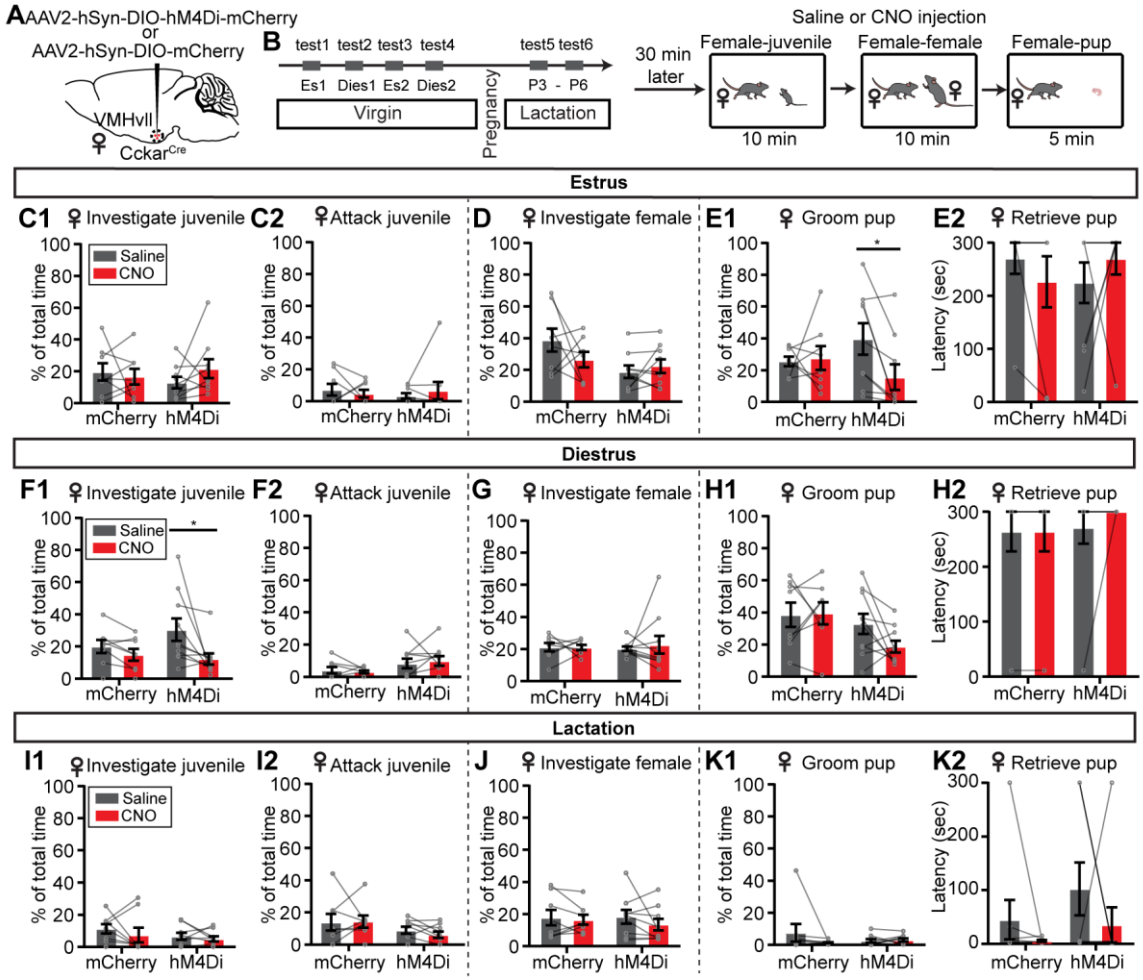

Figure S7. Inactivation of VMHvll^{Cckar} cells causes minimal change in social behaviors towards juveniles, females acnd pups. Related to Figure 2

(A) Viral strategy for chemogenetic inhibition of female VMHvll^{Cckar} cells.

(B) Timeline of the behavioral test.

(C-E) In estrous female, inhibiting VMHvll^{Cckar} cells did not change the percentage of time female spent on investigating juveniles (C1), attacking juveniles (C2), and investigating females (D).

(E) VMHvll^{Cckar} cell inhibition slightly decreased the percentage of time female spent on grooming pups (E1) but did not change the latency of pup retrieval (E2).

(F-H) In diestrous females, inhibiting VMHvll^{Cckar} cells decreased the percentage time animal spent on investigating juveniles (F1), but did not change any other behaviors towards the females, juveniles and pups.

(I-K) In lactating females, inhibiting VMHvll^{Cckar} cells did not change any behaviors towards juveniles, females and pups.

Data are mean ± s.e.m. (C1-K2) Two-way ANOVA with Sidak's multiple comparisons test. *p<0.05.
n = number of animals. n=8 for mCherry group, and n=9 (C-E), 10 (F-H), 9 (I-K) for hM4Di group.

Figure S8

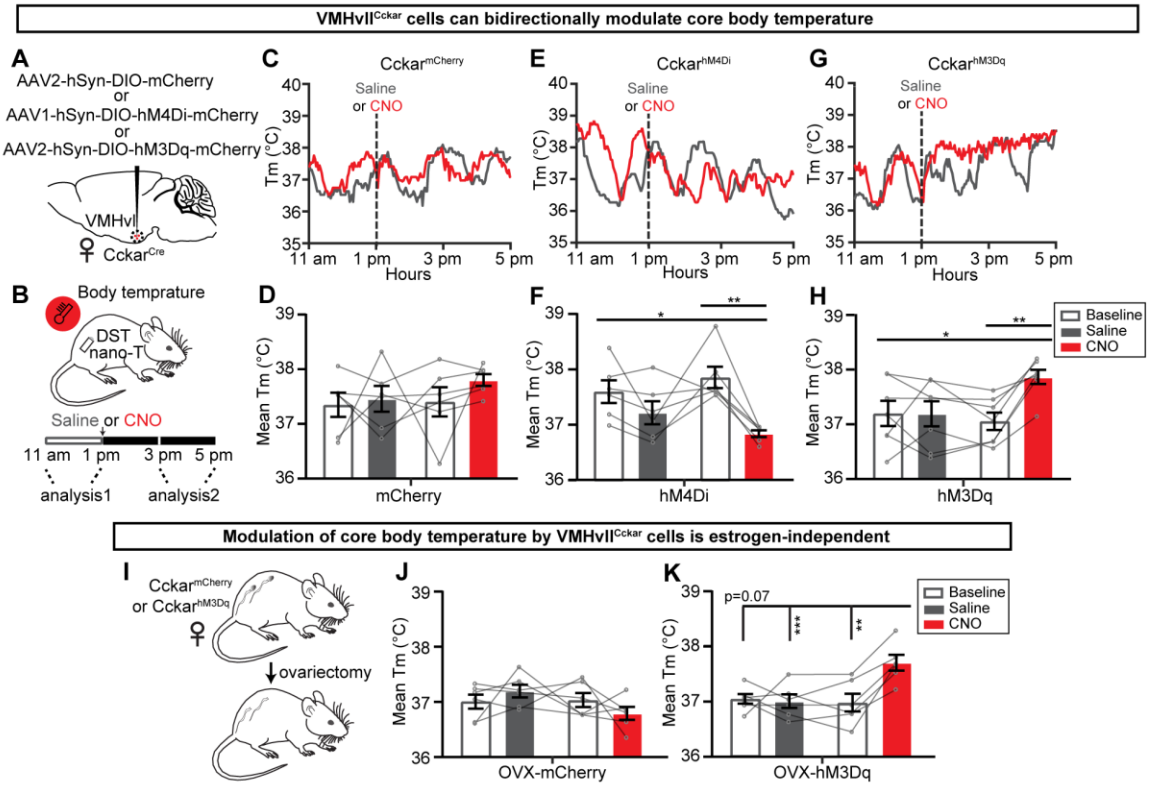

Figure S8. VMHvlI^{Cckar} cells show estrogen-independent bi-directional modulation of core body temperature. Related to Figures 2 and 4

(A) Viral strategy to chemogenetically inhibit or activate VMHvl^{Cckar} cells.

(B) Illustration of chronic body temperature monitoring and the timing of saline or CNO injection. Nano-T logger is implanted in the abdominal cavity and attached to the inside of the body wall.

(C, E, G) Core body temperature from representative Cckar^{mCherry} (C), Cckar^{hM4Di} (E), Cckar^{hM3Dq} (G) female mice, between 11 am to 5 pm, before and after saline or CNO injection at 1 pm.

(D, F, H) Quantification of the mean core body temperature in Cckar^{mCherry} (D), Cckar^{hM4Di} (F), Cckar^{hM3Dq} (H) female mice. Two hours (11 am-1 pm) in baseline and two hours (3 pm to 5 pm) post-saline or CNO injection were used for calculation.

(I) Ovariectomy on Cckar^{mCherry} and Cckar^{hM3Dq} females.

(J-K) Quantification of the mean core body temperature in OVX-Cckar^{mCherry} (J) and OVX- Cckar^{hM3Dq} females (K). Two hours (11 am-1 pm) in baseline and two hours (3 pm to 5 pm) after saline or CNO injection were used for data analysis.

Data are mean ± s.e.m. (D, F, H, J and K) RM one-way ANOVA with Tukey's multiple comparisons test. *p<0.05; **p<0.01; ***p<0.001.

n = number of animals. n=6 (D, F, J, K) and 7 (H) females.

Figure S9

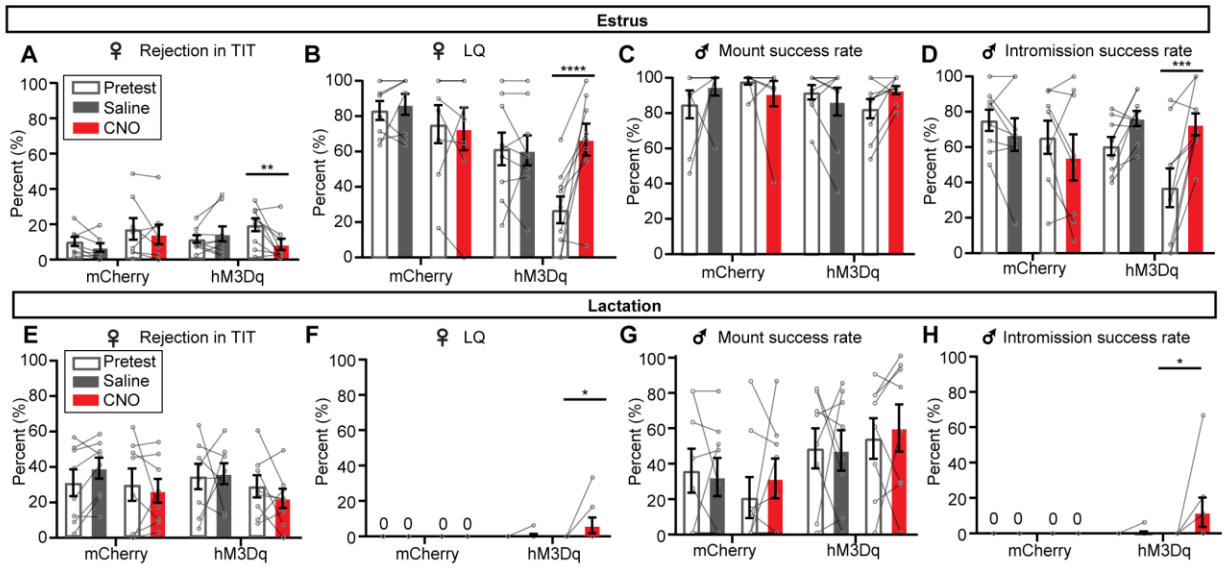

Figure S9. Chemogenetic activation of VMHvll^{Cckar} cells promotes sexual behaviors effectively in estrous females, but only minimally in lactating females. Related to Figure 4

(A-D) In estrous female, activating VMHvll^{Cckar} decreased the percentage of total interaction time females spent on rejecting the males (A), increased lordosis quotient (B), did not change male mount success rate (C), and increased male intromission success rate (D).

(E-H) same as (A-D) but in lactating females.

Data are mean ± s.e.m. (A-H) Two-way ANOVA with Sidak's multiple comparisons test. *p<0.05; **p<0.01; ***p<0.001; ****p<0.0001.

n = number of animals. mCherry: n=8 (A-D) and 8 (E-H); hM3Dq: n=9 (A-D) and 8 (E-H) females.

Figure S10

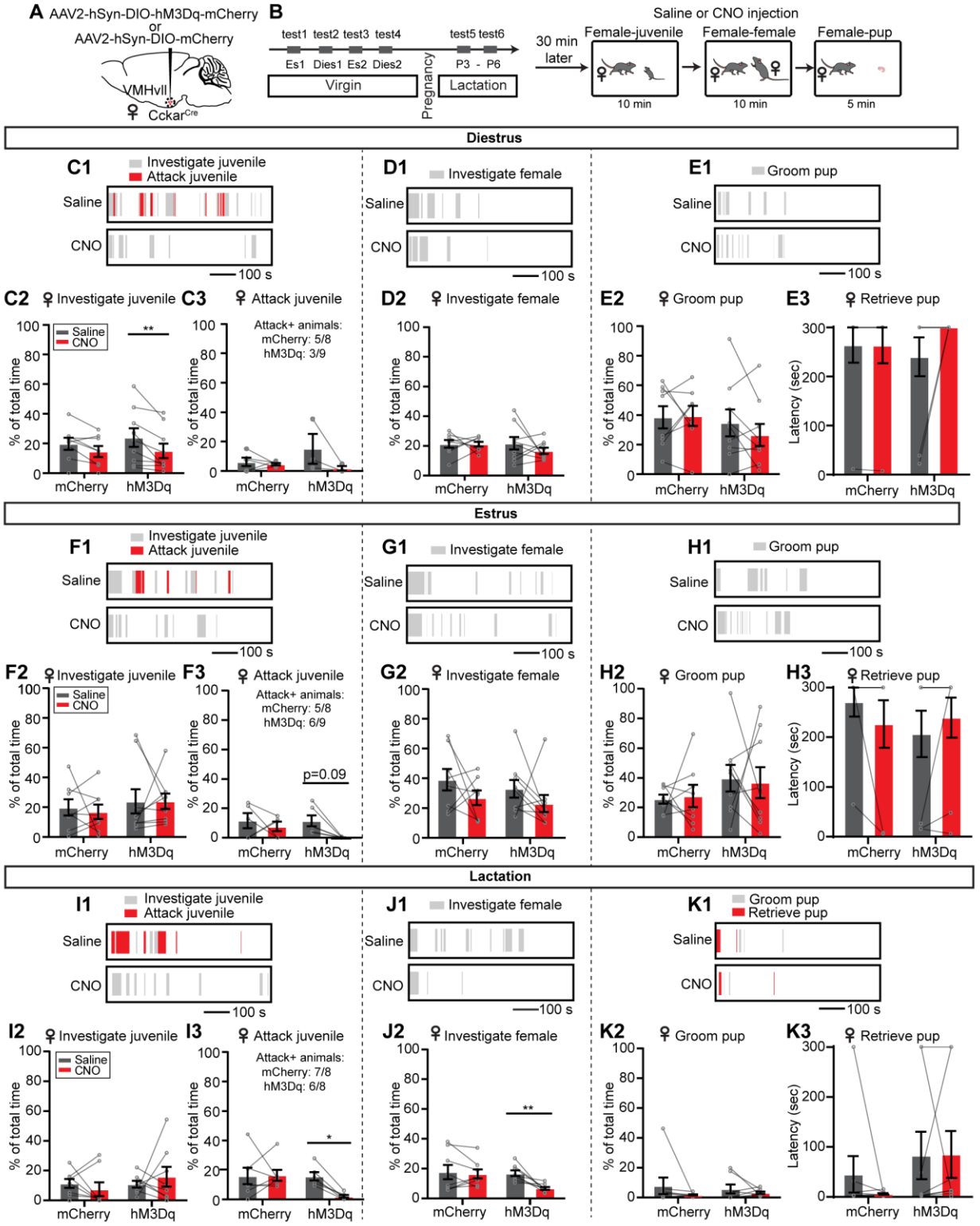
A AAV2-hSyn-DIO-hM3Dq-mCherry
or
AAV2-hSyn-DIO-mCherry
VMHvll
Cckar Cre
B
test1 test2 test3 test4
test5 test6
Es1 Dies1 Es2 Dies2
P3 - P6
Virgin
Pregnancy
Lactation
30 min later
Saline or CNO injection
Female-juvenile
Female-female
Female-pup
10 min
10 min
5 min
Diestrus
C1
Investigate juvenile
Attack juvenile
Saline
CNO
100 s
D1
Investigate female
E1
Groom pup
C2 ♀ Investigate juvenile
C3 ♀ Attack juvenile
Attack+ animals:
mCherry: 5/8
hM3Dq: 3/9
D2 ♀ Investigate female
E2 ♀ Groom pup
E3 ♀ Retrieve pup
% of total time
Latency (sec)
mCherry
hM3Dq
Estrus
F1
G1
H1
F2 ♀ Investigate juvenile
F3 ♀ Attack juvenile
Attack+ animals:
mCherry: 5/8
hM3Dq: 6/9
p=0.09
G2 ♀ Investigate female
H2 ♀ Groom pup
H3 ♀ Retrieve pup
Lactation
I1
J1
K1
Groom pup
Retrieve pup
I2 ♀ Investigate juvenile
I3 ♀ Attack juvenile
Attack+ animals:
mCherry: 7/8
hM3Dq: 6/8
J2 ♀ Investigate female
K2 ♀ Groom pup
K3 ♀ Retrieve pup

Figure S10. Chemogenetic activation of VMHvll^{Cckar} cells suppresses female aggression. Related to Figure 4

(A) Viral strategy for chemogenetic inhibition of female VMHvll^{Cckar} cells.

(B) Timeline of the behavioral test.

(C1) Raster plots showing the behaviors of a diestrous Cckar^{hM3Dq} female towards a male juvenile intruder after saline or CNO i. p. injection.

(C2 and C3) After CNO injection, diestrous Cckar^{hM3Dq} females spent less percentage of time investigating juveniles (C2). Time spent on attacking juvenile also showed a trend of decrease (C3).

(D) Representative raster plots (D1) and bar plots (D2) showing diestrous Cckar^{hM3Dq} females do not change investigation time towards an adult female intruder after VMHvll^{Cckar} cell activation.

(E) Representative raster plots (E1) and bar plots (E2 and E3) showing diestrous Cckar^{hM3Dq} females do not change the percentage of time spent on grooming pups (E2) and the latency of pup retrieval (E3) after VMHvll^{Cckar} cell activation.

(F-H) follow the conventions as in (C-E) showing results in estrous females. Activation of VMHvll^{Cckar} cells in estrous females suppressed female aggression towards juveniles without affecting adult female- and pup-directed behaviors.

(I-K) follow the conventions as in (C-E) showing results in lactating females. Activation of VMHvll^{Cckar} cells in lactating females suppressed female aggression towards juveniles and adult female-directed investigation without affecting pup-directed behaviors.

Data are mean ± s.e.m. (C-K) Two way ANOVA followed by Sidak's multiple comparisons test. *p<0.05; **p<0.01.

n = number of animals. mCherry: n=8 for females in each reproductive state. hM3Dq: n=9, 9, 8 females in diestrus, estrus and lactation, respectively. For juvenile-attacking experiment, only females showed natural aggression were included for analysis. mCherry: n=5, 5, 7 (C3, F3, I3), and hM3Dq: n=3, 6, 6 (C3, F3, I3).

Figure S11

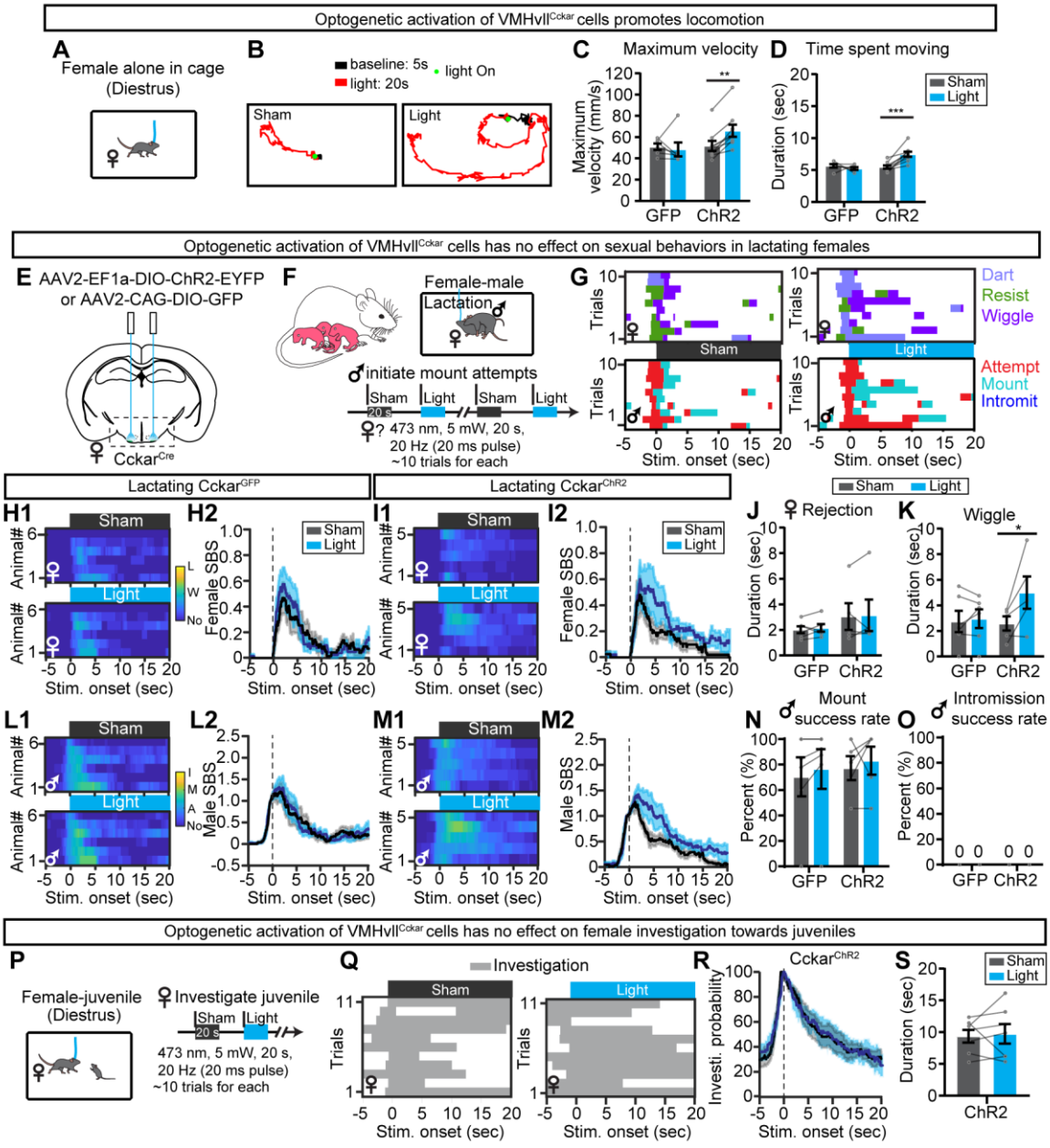

Figure S11. Additional behaviors by optogenetic activation of VMHvlI^{Cckar} cells under different reproductive states. Related to Figure 5

(A) Female was alone in its homecage during light stimulation.

(B) Representative movement trajectories before (5 s, black) and during (20 s, red) sham and light stimulation when a Cckar^{ChR2} female was alone in the home cage. Green dot: sham or light onset.

(C-D) Maximum velocity (C) and time in moving (D) during sham and light stimulation periods in Cckar^{GFP} and Cckar^{ChR2} groups.

(E) Viral strategy to optogenetically activate female VMHvll^{Cckar} cells.

(F) Behavioral paradigm and stimulation protocol. Light/Sham stimulation started when male attempted to mount the lactating test female.

(G) Raster plots showing female (top) and male (bottom) behaviors between a lactating Cckar^{ChR2} female and a sexually experienced male during sham and light stimulation delivered to the female.

(H) Heatmaps (H1) and PSTHs (H2) showing female SBS aligned to sham or light onset of all lactating Cckar^{GFP} females. L: lordosis; W: wiggle: No: no mating.

(I) Heatmaps (I1) and PSTHs (I2) showing female SBS aligned to sham or light onset of all lactating Cckar^{ChR2} females.

(J) The average duration females spent on rejecting the male during light and sham stimulation of Cckar^{GFP} and Cckar^{ChR2} females.

(K) The average duration of wiggling during light and sham stimulation of Cckar^{GFP} and Cckar^{ChR2} females.

(L) Heatmaps (L1) and PSTHs (L2) showing male SBS aligned to the onset of sham or real light delivered to the paired lactating Cckar^{GFP} females. I: intromission; M: mount: A: attempt to mount; No: no mating.

(M) Same as (L) except that the males were paired with lactating Cckar^{ChR2} females.

(N and O) Male mount success rate (N) and intromission success rate (O) during sham and light trials when the males were paired with Cckar^{GFP} or Cckar^{ChR2} females.

(P) Behavioral paradigm and illustration of stimulation protocol. Light was triggered manually when diestrous females were investigating a male juvenile intruder (P15-P25).

(Q) Raster plots showing female investigation towards a juvenile during sham and light trials from a representative Cckar^{ChR2} female.

(R) PSTHs showing female investigation probability aligned to sham or light onsets of all Cckar^{ChR2} females.

(S) The average duration females spent on investigating the juvenile in sham and light trials.

Data are mean ± s.e.m. (H2, I2, L2, M2, R) Two-way ANOVA with repeated measures, followed by Sidak's multiple comparisons test. All $p>0.05$. (C-D, J-K, N) Two-way ANOVA with Sidak's multiple comparisons test. (S) Two-tailed paired t test. *$p<0.05$; **$p<0.01$; ***$p<0.001$.

n = number of animals. GFP: n=6 (C-D), n=6 (H-O); ChR2: n=9 (C-D), n=5 (H-O). n=7 (R-S).

Figure S12

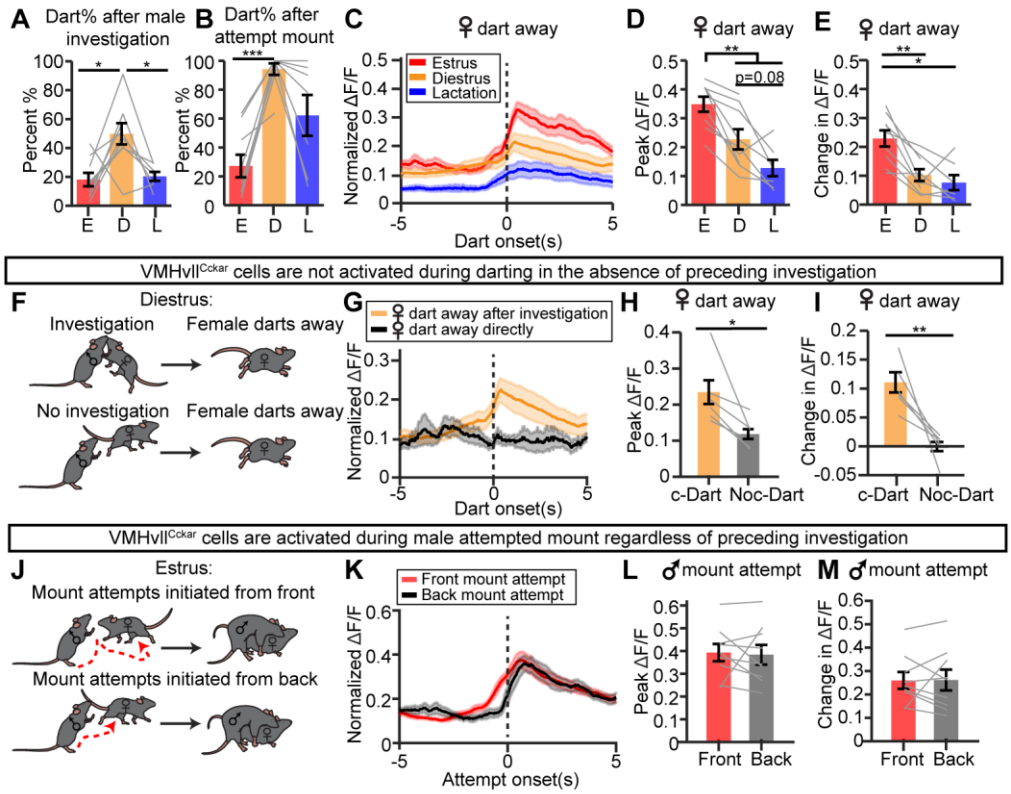

Figure S12. Additional details regarding responses of female VMHvlI^{Cckar} cells during male-female interaction. Related to Figure 6

(A-B) The percentage of male investigation trials (A) and attempt mounting trials (B) that are followed by female darting away from the male when the female is under different reproductive state. E: estrus; D: diestrus; L: lactation.

(C) PETHs of normalized ΔF/F aligned to the onset of female darting.

(D) Quantification of the peak ΔF/F during female darting.

(E) The difference between peak ΔF/F and baseline ΔF/F preceding darting (-3 and -1 s before darting onset).

(F) Schematics illustrating darting events preceded by male-female investigation (top) or not (bottom).

(G) PETHs of normalized ΔF/F aligned to the onset of female darting preceded by male investigation (orange) or not (black).

(H) Peak ΔF/F during female darting. c-Dart: Dart following contact. Noc-Dart: dart with no contact.

(I) Difference between peak ΔF/F and the mean ΔF/F between -3 and -1 s preceding darting.

(J) Schematic illustration of male attempts to mount from front following investigation (top) and male attempts to mount from back without investigation (bottom). Dashed red lines indicate the movement trajectory of the male under these two mounting scenarios.

(K) PETHs of normalized ΔF/F aligned to the onset of male front mounting attempts (red) and back mounting attempts (black).

(L) Peak ΔF/F during male front and back mounting attempts.

(M) The difference between peak ΔF/F and baseline ΔF/F preceding attempted mount (-3 and -1 s before the attempt onset).

Data are mean ± s.e.m. (A, B, D, E) One-way ANOVA with repeated measures, followed by Tukey's multiple comparisons test. (H, I, L, M) Two-tailed paired t test. *p<0.05; **p<0.01; ***p<0.001.

n = number of animals. (A-E) n=9 estrous, 9 diestrous and 7 lactating females. (G-I) n= 6 diestrous females. (K-M) n=9 estrous females.

Figure S13

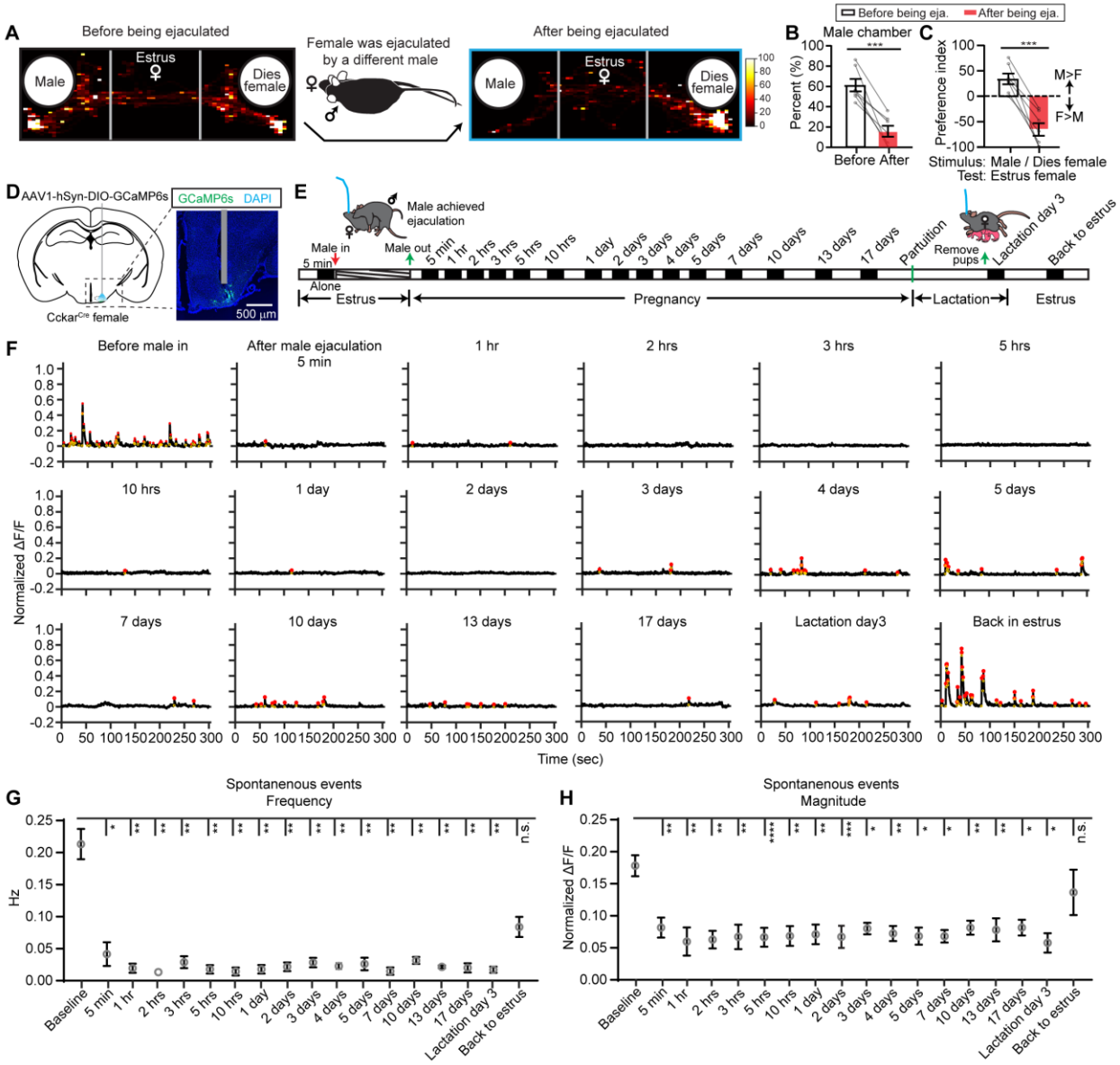

Figure S13. Changes in female's interest towards males and spontaneous Ca^{2+} transients of female VMHvll^{Cckar} cells after being ejaculated. Related to Figure 6

(A) Heatmap showing the distribution of female's body center location in a social preference test before and after being ejaculated. The test animal is an estrous-receptive female. Stimulus animals are a sexually experienced unfamiliar male (different from the one that copulated with the female) and an unfamiliar diestrous female.

(B) Percent of time female spent in male's chamber before and after being ejaculated.

(C) Comparison of preference index (PI) in females before and after being ejaculated. Positive values indicate male preference.

(D) Schematics illustrating fiber photometry recording of VMHvll^{Cckar} cells and representative histology image showing the expression of GCaMP6s in VMHvll^{Cckar} cells. Shade indicates optic fiber track.

(E) Timeline of the pre- and post-ejaculation recordings. Each recording session lasts 5 minutes.

(F) Representative traces from all recorded time points from one representative animal. Red and yellow dots indicate peaks and troughs of identified transients.

(G-H) Frequency (G) and magnitude (H) of spontaneous Ca^{2+} events before and after male ejaculation.

Data are mean ± s.e.m. (B-C) Two-tailed paired t test. (G-H) RM One-way ANOVA, followed by Dunnett's multiple comparisons test. *p<0.05; **p<0.01; ***p<0.001.

n = number of animals. n=7 (B-C), n= 6 (G-H) females.

Figure S14

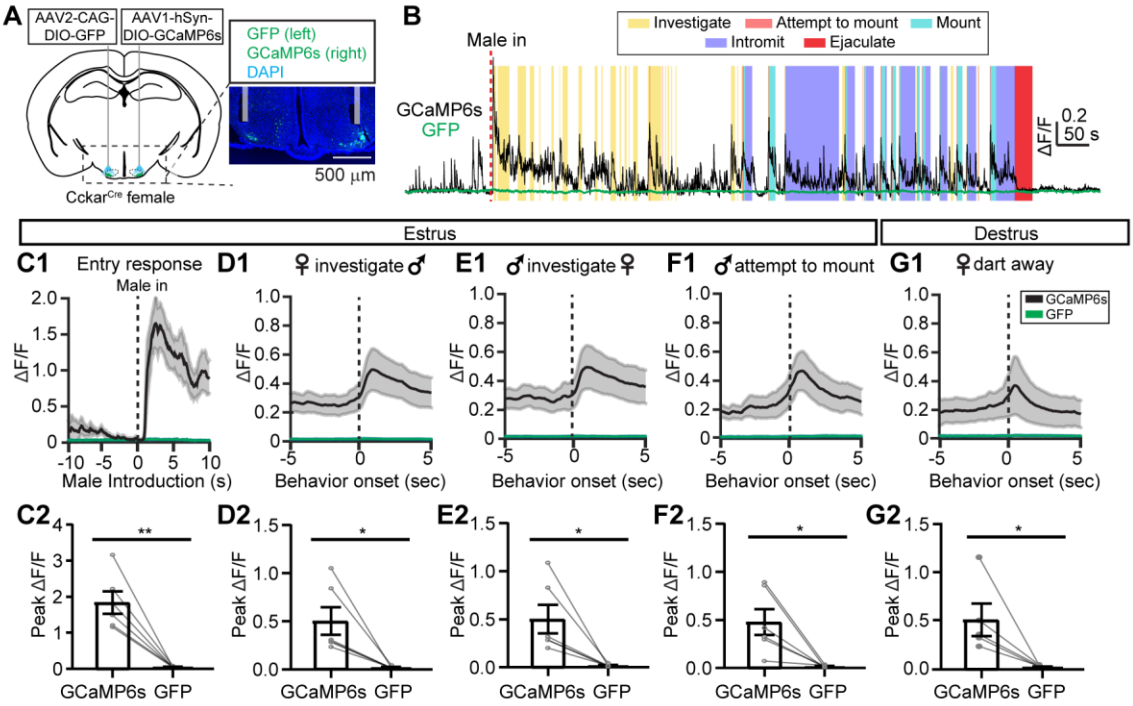

Figure S14. GFP expressing VMHvll^{Cckar} cells show no change in fluorescence during female sexual behaviors. Related to Figure 6

(A) Viral strategy and a representative image showing GFP and GCaMP6s expression and fiber tracks.

(B) Representative ΔF/F GFP (green) and GCaMP6s (black) traces during copulation with a male. Colored shades mark behavioral episodes.

(C1-G1) PETHs of GFP and GCaMP6s signals aligned to the onset of various behaviors from all recording animals.

(C2-G2) Peak signal of GFP and GCaMP6s PETHs aligned to the onsets of male introduction (C2), female investigating male (D2), male investigating female (E2), male attempting to mount (F2), and female darting away (G2).

Data are mean ± s.e.m. (C2, F2 and G2), Two-tailed paired t test. (D2 and E2), Two-tailed Wilcoxon matched-pairs signed rank test. *p<0.05; **p<0.01;

n = number of animals. n=6 (C2-F2) and n= 5 (G2) females.

Figure S15

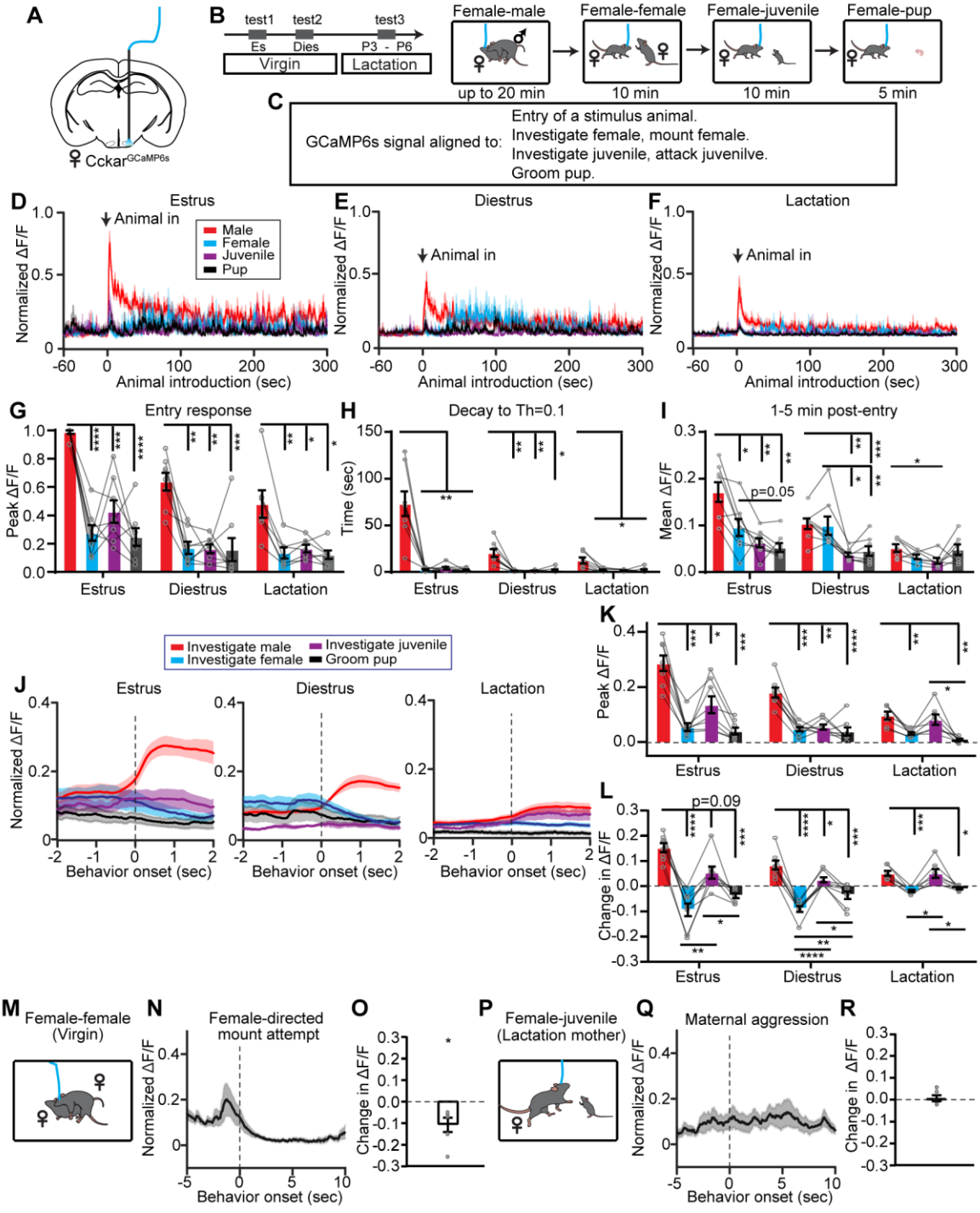

Figure S15. Responses of VMHvll^{Cckar} cells during interactions with females, juveniles and pups. Related to Figure 6

(A) Schematics illustration of fiber photometry recording of female VMHvll^{Cckar} cells.

(B) Schematic illustration of the recording protocol.

(C) Main parameters analyzed in the figure.

(D-F) PETHs of normalized ΔF/F aligned to the introduction of various social stimuli. Each trace is the averaged PETHs of all recorded females in estrus (D), diestrus (E) and lactation (F).

(G) Peak ΔF/F within the first 60 s after male entry.

(H) Upon stimulus animal introduction, the decay time for the normalized ΔF/F to reach 0.1 after peaking

(I) Mean ΔF/F from 1-5 minutes after stimulus animal introduction.

(J) PETHs of normalized ΔF/F aligned to the onset of investigating male, investigating female, investigating juvenile and grooming pup. Each trace is the average of all recorded females in estrus (left), diestrus (middle) and lactation (right).

(K) Peak ΔF/F during various behaviors under different reproductive states.

(L) Difference between the peak ΔF/F during the behavior and the mean ΔF/F between -3 and -1 sec before the behavior onset.

(M) Cartoon showing female-female mounting.

(N) Average PETH of normalized ΔF/F aligned to the onset of female-directed mounting attempt.

(O) Change in ΔF/F during female mounting attempt from the baseline ΔF/F (-3 and -1 sec) preceding the onset of mount attempt.

(P) Carton showing a lactating female attacking a juvenile intruder.

(Q) Average PETH of normalized ΔF/F aligned to the onset of attacking juvenile.

(R) Difference between the peak ΔF/F during attacking juvenile and the mean baseline ΔF/F (-3 and -1 sec) preceding the attack onset.

Data are mean ± s.e.m. (G-I, K-L) Two-way ANOVA with Tukey's multiple comparisons test. (O) One sample Wilcoxon signed-rank test, with hypothetical value as 0. (R) One sample t test, with hypothetical value as 0. *p<0.05; **p<0.01; ***p<0.001.

n = number of animals. (D-L): n=8 estrous, 8 diestrous and 7 lactating females. (O): n=6 virgin females. (R): n = 6 lactating females.

Figure S16

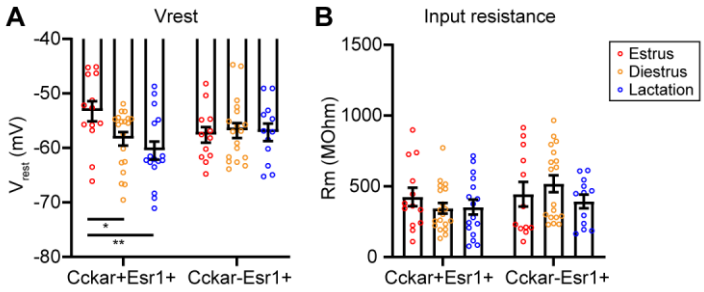

Figure S16. VMHvll^{Cckar} cells show more depolarized resting membrane potential during estrus. Related to Figure 8

(A-B) The resting membrane potential (A) and input resistance (B) of VMHvll$^{Cckar+Esr1+}$ and VMHvll$^{Cckar-Esr1+}$ cells recorded from females under different reproductive states.

Data are mean ± s.e.m. (A-B) Two way ANOVA followed by Tukey's multiple comparisons test. *p<0.05; **p<0.01.

N=13, 19, 16 VMHvll$^{Cckar+Esr1+}$ cells and 12, 18, 12 VMHvll$^{Cckar-Esr1+}$ cells from 3 females of each reproductive state. Cells with high spontaneous firing rate were excluded from these analyses.

Figure S17

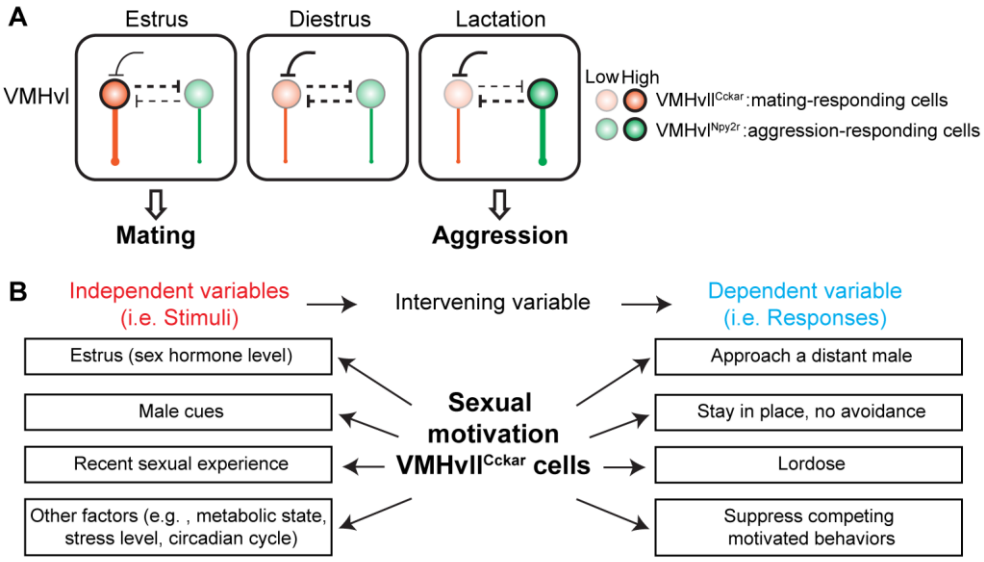

Figure S17. Working model and VMHvll^{Cckar} cells as the intervening variable in the reproduction circuit. Related to Figures 1-8

(A) A model showing our current knowledge regarding the neural mechanisms underlying behavior change across reproductive states. During estrus, VMHvll^{Cckar} cells receive lower inhibitory inputs, increase excitability and axonal arborization to increase the cell output in response to male cues and facilitate female sexual behaviors. In lactating females, VMHvll^{Cckar} cells become less responsive due to changes at input, output and cellular levels while responses of VMHvl^{Npy2r} cells increase to facilitate aggression.

(B) We propose VMHvll^{Cckar} cells as the physical embodiment of sexual motivation, an intervening variable linking different stimuli (independent variables) and many different behavior responses (dependent variables). The figure follows the format of Figure 1 in (Andermann and Lowell, 2017) that describes hunger and AGRP cells as an intervening variable for controlling feeding.